Ray-Tracing Simulations of the 60 GHz Incabin Radio Channel

***Robert Felbecker*, Wilhelm Keusgen, Michael Peter**

Fraunhofer-Institut für Nachrichtentechnik, Heinrich-Hertz-Institut, Einsteinufer 37, 10587 Berlin, Germany
Phone: +49 30 31002-{672, 639, 583},
e-mail: {robert.felbecker, wilhelm.keusgen, michael.peter}@hhi.fraunhofer.de

Abstract

In this paper, we present first results of ray-tracing simulations of the 60 GHz in-vehicular radio channel. The simulations have been performed with respect to the passenger cabin of a wide-bodied aircraft. A very detailed 3D model of the cabin has been drawn up. Parameters of common materials were taken from literature. Unknown values have been determined by means of free space measurements. For composite materials we made the approach of defining an effective dielectric constant and an effective thickness. The simulation results have been analyzed regarding small-scale fading behavior, path loss and delay spread.

1. Introduction

During the last years the implementation of wireless cabin infrastructure attracts much interest for both manufacturers and airlines. Therefore, the research for wireless communication systems capable of providing broadband communication is in full progress. The inflexibility of wired systems, the weight of the cables and therefore, the overall costs are strong arguments for investigations on flexible and lighter wireless systems. Nevertheless, a wireless system must ensure the same security levels and quality of service requirements and must be able to be used worldwide without the burden of license fees. Approaches using the ISM-Bands at 2.4 GHz resp. at 5.2 GHz will almost certainly not be able to reach these requirements due to insufficient bandwidth especially with respect to the transmission of multi-media data to all passengers in a wide-bodied aircraft. In order to avoid these problems, the 60 GHz approach looks promising, since several GHz of unlicensed bandwidth are expected to be recently available worldwide and interference to electronic equipment is naturally very small.

A basic requirement for the realization of each wireless communication system is the knowledge of the underlying radio channel. Possibilities to obtain information of the radio channel are channel measurements and the deterministic calculation of the wave propagation. Although investigations on 60 GHz communication has been done for years now [1], little work has been done regarding the investigation of the broadband incabin radio channel and high-resolution ray-tracing investigations have not been performed so far to the best knowledge of the authors. In this paper, a ray-tracing method is used to investigate the radio wave propagation in the millimeter wave band. For the simulations a detailed model of a part of the passenger cabin of a wide-bodied aircraft has been drawn up. Since only few information about material parameters in the millimeter band is available from the literature, the values of special materials like carbon fiber reinforced plastic (CRP) and glass fiber reinforced plastic (GRP) have been estimated from reflection and transmission measurements.

2. Ray-Tracing Tool and 3D Model

Ray-tracing based on geometrical optics offers some advantages over channel measurements like an infinite signal-to-noise-ratio (SNR) and an unlimited temporal resolution of paths. Recent channel measurements in the 60 GHz frequency range provide a maximum measurement bandwidth of about 1 GHz, which results in a temporal resolution of 1 ns [2, 3]. This limited resolution leads to the effect, that paths with a delay smaller than 1 ns relative to each other cause fading. The unlimited temporal resolution of paths found on the basis of ray-tracing may give a better understanding of the aforementioned fading effect. The used ray-tracer (RT) implements ray-launching as ray-tracing algorithm and uses ray-imaging to determine the exact reflection point and hence the correct amplitude and phase of already traced paths. It models the main propagation effects such as specular reflection and transmission. The effects of scattering and diffraction have been neglected for the simulations, since all surfaces have been regarded as flat in relation to the wavelength and because of the small impact diffracted rays have at high frequencies.

Regarding the small wavelength of 5 mm a very detailed model for the ray-tracing simulations has been drawn up. The physical dimensions of the modeled passenger cabin are approximately 12 m in length, 1.9 m in height and 6 m in width. Fig. 1 gives an impression of the 3D model. The material parameters used for the model have been taken partly from literature, as for example the permittivity of plastic. The material parameter of other materials like CRP and GRP have been extracted out of free space measurements with a method similar to those in [4, 5]. As these two materials are not homogeneous their estimated ϵ_r and thickness are effective values.

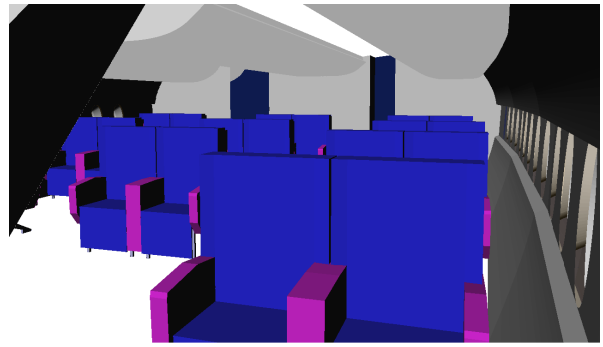

Fig. 1: 3D model of the passenger cabin.

Tab. 1 gives an overview of involved materials and their respective complex ϵ_r and thickness D. The CRP-parts cover the floor and some parts of the ceiling, the GRP-parts were used to model the wall panels, most ceiling panels and the overhead lockers. The windows, which are metallized, have been modeled as perfect electric walls. Transmission measurements with office chairs surprisingly have shown that the cushioning of chairs is highly transmissive and has an ϵ_r very close to that of air. Therefore, the cushioning has not been taken into account, but the plastic frame of the seats and its metallic parts have been modeled. Nevertheless the situation may become different with passengers.

Material	$\epsilon_r^{'}$	$\epsilon_r^{''}$	D
Plastic [6]	2.25	0.0009	0.01
Metallized glass	-	-	-
Material	$\epsilon_{r,\text{eff}}^{'}$	$\epsilon_{r,\text{eff}}^{''}$	D_{eff}
CRP	4.1	0.07	0.004
GRP	8.7	0.26	0.0028

Table 1: Material parameters used in the RT.

3. Simulation Settings

To get a good insight in the characteristics of the 60 GHz incabin channel the propagation behavior with respect to small-scale fading and large-scale fading has to be analyzed. For these two fading effects different simulation setups were regarded. In both setups the transmitter (Tx) had a fixed position at the side of the inner cabin hull at a height of 1.6 m comparable to the setup described in [2]. In the case of the large-scale simulations a rectangular grid of receivers was positioned in the x-y-plane with a receiver (Rx) spacing of 10 cm (20 wavelengths). For the calculation of the path loss isotropic antennas were assumed both for the Rx and the Tx. The same antenna configuration was used to extract a reference value of the channel's delay spread. In order to obtain a realistic value for the delay spread, which is comparable to measurement results, an open-ended waveguide antenna (dimension: WR15, gain 8 dBi) was applied as transmitter. When wanting to get more detailed knowledge on which paths exactly interact, causing the effect of small-scale fading, ray-tracing offers the possibility to simulate the channel with unlimited bandwidth. To reproduce the small-scale fading effect a receiver spacing smaller than $\lambda/2$ has to be maintained, therefore at distinct positions lines of receivers with a spacing of 1 mm have been set up. Each of these lines consists of 100 receive points and 14 of such small-scale sets were simulated at the back of the seats related to the positions of the broadband channel measurements reported in [2]. In order to get accurate results, the number of allowed interactions with surfaces has to be adequate. With the method proposed by [7] the total number of allowed interactions was set to 6 reflections and 4 transmissions.

4. Simulation Results

A ray-tracing tool delivers a prediction of the complex channel impulse response (CIR) for each receive point, taking into account the patterns of the transmitting and the receiving antenna. The CIR $h(\tau)$ is described by

$$h(\tau) = \sum_{k=0}^{K-1} a_k \exp(j\phi_k)\delta(\tau - \tau_k), \tag{1}$$

where a_k, ϕ_k, τ_k are the amplitude, the phase and the delay of the k-th propagation path, respectively.

Assuming isotropic antennas, the path loss PL can be calculated on the basis of the path amplitudes by

$$\mathrm{PL} = \frac{1}{\sum_{k=0}^{K-1} |a_k|^2}. \tag{2}$$

Fig. 2 shows the scatter plot of the predicted path loss as a function of distance between Tx and Rx. In addition, the linear regression line resulting from a least-squares approximation is shown. We obtain a path loss exponent of $n = 1.59$ and an intercept point of $\overline{\mathrm{PL}}(d_0 = 1\ \mathrm{m}) = 67.2$ dB according to the path loss exponent model [8]

$$\overline{\mathrm{PL}}(d)[\mathrm{dB}] = \overline{\mathrm{PL}}(d_0)[\mathrm{dB}] + 10n \cdot \log_{10}\left(\frac{d}{d_0}\right), \tag{3}$$

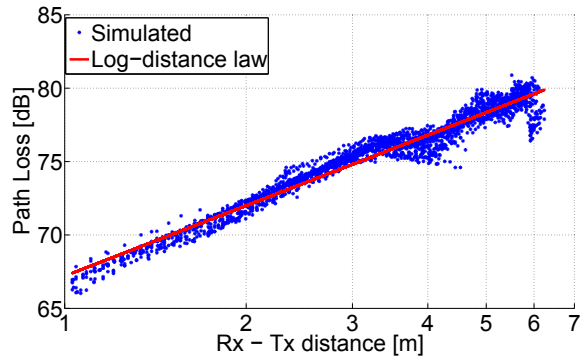

Fig. 2: Path loss versus distance between Tx and Rx.

where d denotes the distance between the Tx and the Rx. The results are very close to the measured values in [2].

The RMS delay spread is a common measure to characterize the time dispersion of a multipath channel. With $\tau_0 = 0$ it is given by

$$\tau_{\mathrm{rms}} = \sqrt{\frac{\sum_{k=0}^{K-1} \tau_k^2 \cdot a_k^2}{\sum_{k=0}^{K-1} a_k^2} - \tau_{\mathrm{m}}^2} \quad \text{with} \quad \tau_{\mathrm{m}} = \frac{\sum_{k=0}^{K-1} \tau_k \cdot a_k^2}{\sum_{k=0}^{K-1} a_k^2}. \tag{4}$$

The cumulative distribution of τ_{rms} is illustrated in Fig. 3 for both antenna configurations. In order to obtain values that could be compared to the measurement results in [2], an additional evaluation was made by involving only paths within a certain delay window. The window results from applying a -30 dB threshold relative to the strongest path. The median delay spread is around 10 ns for both antenna configurations. A slightly higher delay spread is obtained for the analysis without the threshold. Hence some paths with longer delays beneath the threshold still contribute to the delay spread, but do not change it significantly. The difference between the behavior of the curves of the two antenna configurations can be explained as follows: on the one hand the directivity of the open-ended waveguide leads to smaller delay spreads if the receive point is situated in the direction of the main beam. On the other hand smaller spreads can arise from significantly differing directions. The overall average value of τ_{rms} is 10.0 ns and only slightly larger than for the measurements in [2], where a value of 8.6 ns has been determined.

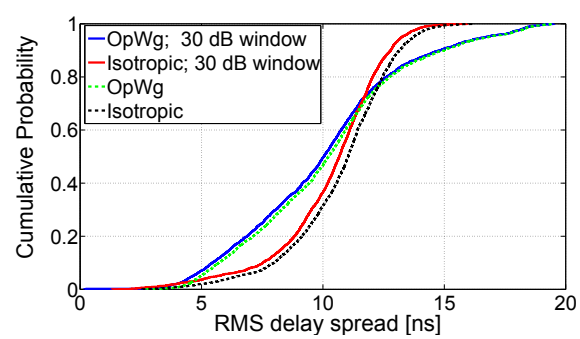

Fig. 3: Cumulative distribution of the RMS delay spread.

In order to investigate the spatial small-scale characteristics of the channel and the impact on a practical system, the CIRs of the small-scale simulations were bandlimited by applying a Kaiser window with $\beta = 5$ with a total bandwidth of 1 GHz. Fig. 4 illustrates an exemplary set of simulated CIRs for 100 receive points obtained from a receiver location with a Tx-Rx distance of approximately 6 m. The effect of small-scale fading is clearly visible, but there are also several strong paths besides the LOS component which do not fade significantly. Backtracing of the strongest multipaths revealed that they result from reflections at the metallized windows. Comparable effects were observed in [2] and could now be explained by the simulations. On the other side it seems that in general the fading of multipaths is stronger for the measurement results than for the simulations. A possible explanation for this fact is that scattering was not considered. Additional measurements regarding the scattering behavior of the materials are to be made in order to analyze this.

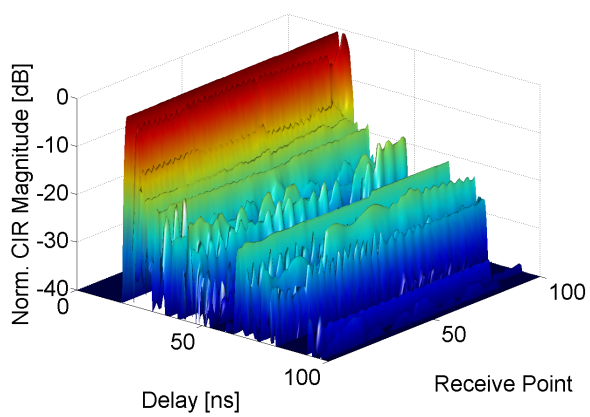

Fig. 4: Exemplary small-scale set of CIRs.

5. Conclusion

In this paper, the 60 GHz incabin broadband channel has been investigated by means of ray-tracing. A detailed 3D model of a wide-bodied aircraft has been drawn up, whereby special care has been taken in including appropriate parameters of involved composite materials. Effective dielectric constants and thicknesses have been determined on the basis of reflection and transmission measurements. The model was used to perform simulations with regard to large-scale and small-scale evaluations, namely path loss, delay spread and small-scale fading behavior. The results show a good match with the measurement results in the same environment [2]. The appearance of strong paths especially arising from reflections at the windows is also consistent with the measurement results. However, the small-scale channel characteristics could not be predicted precisely and further work has to be done to investigate the practical impact of scattering in an incabin scenario. Finally the influence of passengers should be analyzed.

6. Acknowledgements

The authors would like to thank Prof. Dr. Ing. Bernhard Rembold and Dipl. Ing. Patrick Bosselmann from the Institute of High Frequency Technology at the RWTH Aachen University, who provided us with the ray-tracer.

7. References

[1] P. Smulders. Exploiting the 60 GHz band for local wireless multimedia access: prospects and future directions. *Communications Magazine, IEEE*, 40(1):140–147, 2002.

[2] M. Peter, W. Keusgen, A. Kortke, and M. Schirrmacher. Measurement and analysis of the 60 GHz in-vehicular broadband radio channel. In Wilhelm Keusgen, editor, *Vehicular Technology Conference, 2007. VTC-2007 Fall. 2007 IEEE 66th*, pages 834–838, 2007.

[3] T. Zwick, T. J. Beukema, and H. Nam. Wideband channel sounder with measurements and model for the 60 GHz indoor radio channel. *Vehicular Technology, IEEE Transactions on*, 54(4):1266–1277, 2005.

[4] J. P. Pugliese, A. Hammoudeh, and M. Al-Nuaimi. Estimation of dielectric parameters from reflection and transmission coefficients of building materials at 62 GHz. In *Antennas and Propagation, Tenth International Conference on (Conf. Publ. No. 436)*, volume 2, pages 1–4 vol.2, 1997.

[5] B. Langen, G. Lober, and W. Herzig. Reflection and transmission behaviour of building materials at 60 GHz. In *Personal, Indoor and Mobile Radio Communications, 1994. Wireless Networks - Catching the Mobile Future. 5th IEEE International Symposium on*, pages 505–509 vol.2, 1994.

[6] D. M. Pozar. *Microwave Engineering Third Edition*. Wiley, 2005.

[7] M. Peter, W. Keusgen, and R. Felbecker. Measurement and ray-tracing simulation of the 60 GHz indoor broadband channel: Model accuracy and parameterization. In *2nd European Conference on Antennas and Propagation, EUCAP 2007*, 2007.

[8] H. Xu, V. Kukshya, and T. S. Rappaport. Spatial and temporal characterization of 60 GHz indoor channels. In *Vehicular Technology Conference, 2000. IEEE VTS-Fall VTC 2000. 52nd*, volume 1, pages 6–13 vol.1, 2000.